Journal of the Optical Society of America B
OPTICAL PHYSICS

# Ultrasensitive displacement measurement with nonlinear optomechanical coupling and squeezed light injection

Doudou Wang,[1] Quansen Wang,[1] Qiang Zhang,[1,2] and Yongmin Li[1,2,*]

[1]State Key Laboratory of Quantum Optics and Quantum Optics Devices, Institute of Opto-Electronics, Shanxi University, Taiyuan 030006, China
[2]Collaborative Innovation Center of Extreme Optics, Shanxi University, Taiyuan 030006, China
*Corresponding author: yongmin@sxu.edu.cn

Received 16 September 2022; revised 4 December 2022; accepted 12 January 2023; posted 13 January 2023; published 16 February 2023

**We propose an ultrasensitive displacement measurement scheme to overcome the standard quantum limit (SQL) in the unresolved sideband cavity optomechanical system with nonlinear optomechanical coupling and squeezed light injection. By introducing the optimized quantum correlation, which is enabled by suitable choices of the squeezing angle, squeezing level, power of the probe light, and measurement angle of homodyne detection, the off-resonant displacement sensitivity reaches 6 dB below the SQL in linear optomechanical coupling. In contrast, displacement sensitivities with a coherent probe plus variational readout and squeezed probe plus fixed measurement angle (phase quadrature) are 2.6 dB and 4.6 dB below the SQL, respectively. By combining linear and quadratic optomechanical coupling, we show that the displacement sensitivity can be further improved to 9.6 dB below the SQL. Our results have potential applications in gravitational-wave detectors, quantum metrology, and the search for dark matter.** 

https://doi.org/10.1364/JOSAB.475955

## 1. INTRODUCTION

Optical displacement measurement is crucial in various fields such as atomic force microscopy and high-resolution imaging. Displacement sensitivity is limited by the standard quantum limit (SQL) for displacement measurements based on an optical interferometer due to the Heisenberg's uncertainty principle of conjugate quadratures. The SQL derives from the imprecision of the measurement and the quantum backaction [1,2]. Displacement sensitivity has approached or even surpassed the SQL for various systems, such as nano-optomechanical devices [3–5], ultracold atoms [6], Advanced LIGO [7–12], and the search for dark matter [13].

Over the years, a variety of approaches for surpassing SQL have been proposed [1]. The proposed methods can be classified into two types: quantum backaction-evading measurement [14,15] and introduction of quantum correlations between imprecision and backaction [11,16,17]. In the latter case, the SQL may be beaten by designing an appropriate correlation between an object's position (momentum) uncertainty and the photon number (phase) uncertainty of the probe it reflects [11]. Such correlations can be achieved using nonlinear cavities [18] or injecting squeezed light [19–24]. An alternative method is employing optomechanical induced correlations by rotating the readout quadrature of the output probe as a function of frequency [25,26], so called variational readout. In this direction, the off-resonant force and displacement sensitivity better than the SQL have been demonstrated [16,17].

By using phase quadrature squeezed light and readout on phase quadrature, it is shown that the squeezing light hardly improves the motion sensing of resonators in the unresolved sideband region, but may significantly improve measurement sensitivity in the resolved sideband region [27]. To reach higher displacement sensitivity, variational readout with squeezed light was investigated [28]. However, squeezed light with a fixed squeezing angle (amplitude quadrature) is assumed, and the influence of squeezing angle on displacement sensitivity has remained unclear. A recent work [29] proposes a new scheme for approaching the quantum limit. The input and output filter cavities included in the scheme are used for frequency-dependent squeezing and variational readout. Nevertheless, little attention has been paid to the condition of exceeding the SQL.

The mechanical mode and optical mode interact through linear (dispersive) optomechanical coupling (LOC) in conventional optomechanical systems. Later, higher-order nonlinear interactions such as quadratic optomechanical coupling (QOC) arising from the mechanical resonantor's squared displacement was observed [30]. Recently, it was shown that combining LOC and QOC interactions can result in force and displacement sensitivity beyond the SQL [31,32].

In this paper, motivated by the above studies, we consider the combined effect of nonlinear optomechanical interactions (combined LOC and QOC interactions) and squeezed light injection on sensitive displacement measurement. First, we investigate the effects of relevant parameters including the squeezing angle, squeezing level, probe optical power, and readout quadrature on the displacement sensitivity of a mechanical resonator in an unresolved sideband cavity optomechanical system with only LOC. The interplay among these parameters is analyzed in depth. Then, we analyze the sensitive displacement measurement when QOC interaction is introduced. We find that combining squeezed light injection and nonlinear optomechanical interactions significantly improves displacement sensitivity, with a value of 9.6 dB below the SQL.

The paper is organized as follows. In Section 2, we derive the displacement measurement spectrum of the cavity optomechanical system with LOC and squeezed light injection. In Section 3, the effects of the relevant parameters on displacement measurement sensitivity and their interplay are analyzed in depth. In Section 4, we study the combined effect of nonlinear optomechanical interactions (combined LOC and QOC interactions) and squeezed light injection on the displacement measurement. In Section 5, we draw a conclusion.

## 2. DISPLACEMENT MEASUREMENT WITH LOC AND SQUEEZED LIGHT INJECTION

The considered optomechanical setup consists of a Fabry–Perot (F-P) cavity and SiN membrane with squeezed light injection [17,33,34], as shown in Fig. 1. The optical cavity provides a resonant enhancement of the input probe field. The radiation pressure interaction perturbs the motion of the membrane resonator, imprinting its position information on the enhanced intracavity probe field. By properly choosing system parameters, the continuous measurement beyond SQL at the off-resonance frequency of the mechanical oscillator can be achieved.

In the rotating frame of the probe laser field frequency $\omega$, the Hamiltonian of the system can be given by [1]

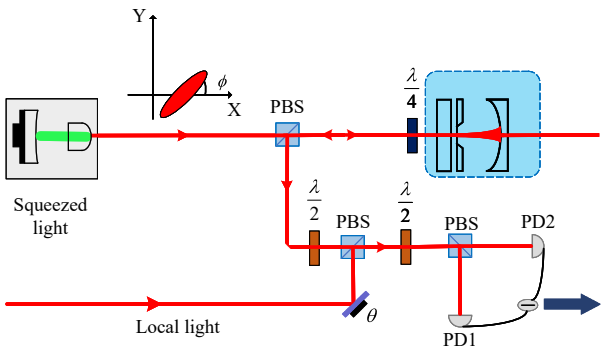


**Fig. 1.** Schematic of the system. PBS, polarizing beam splitter; PD, photodiode; $\phi$, squeezing angle; $\theta$, measurement angle. A beam of bright squeezed light enters the optomechanical system, and the reflected probe light carries the displacement information of the membrane resonator, which can be measured by balanced homodyne detection.

$$\hat{H}=\frac{\hbar\Omega_m}{2}(\hat{Q}^2+\hat{P}^2)-\hbar\Delta\hat{a}^\dagger\hat{a}-\sqrt{2}\hbar g_0\hat{a}^\dagger\hat{a}\,\hat{Q}+i\hbar\sqrt{\kappa_L}(\alpha_{\rm in}\hat{a}^\dagger+\text{c.c}), \tag{1}$$

where $\Omega_m$ is the angular resonance frequency of the harmonic oscillator, $\Delta\equiv\omega-\Omega_c$ is the detuning of the probe laser frequency $\omega$ relative to the cavity resonance frequency $\Omega_c$, $g_0$ is the vacuum optomechanical coupling rate and $\hat{a}(\hat{a}^\dagger)$ is the annihilation (creation) operator of the cavity mode. The first term denotes the energy stored in the mechanical oscillator with dimensionless position operator $\hat{Q}$ and momentum operator $\hat{P}$, which satisfy $[\hat{Q},\hat{P}]=i$. The second term describes the free energy of the cavity, and the third term is the interaction Hamiltonian. The last term denotes the input probe field $\alpha_{\rm in}$, where $\kappa_{\rm L}$ is the decay rate of the cavity of the left mirror, and c.c stands for complex conjugate.

Starting from the quantum Langevin equations, we simulate the dynamics of the system by expanding the field operators as steady-state values and fluctuation terms, where $\hat{a}=\bar{\alpha}+\delta\hat{a}$, $\hat{Q}=Q_s+\delta\hat{Q}$, and $\hat{P}=P_s+\delta\hat{P}$; the linearized quantum Langevin equations for the fluctuations of mechanical and optical modes are given by

$$\begin{aligned}
\delta\dot{\hat{a}}&=-\frac{\kappa}{2}\delta\hat{a}+i\tilde{\Delta}\delta\hat{a}+i\sqrt{2}g\delta\hat{Q}+\sqrt{\kappa_R}\delta\hat{a}_{\text{in},R}+\sqrt{\kappa_L}\delta\hat{a}_{\text{in},L},\\
\delta\dot{\hat{Q}}&=\Omega_m\delta\hat{P},\\
\delta\dot{\hat{P}}&=-\Omega_m\delta\hat{Q}-\Gamma_m\delta\hat{P}+\sqrt{2\Gamma_m}\delta\hat{P}_{\rm in}+\sqrt{2}g(\delta\hat{a}^\dagger+\delta\hat{a}),
\end{aligned} \tag{2}$$

where $\kappa_R$ is the decay rate of the cavity to the right mirror, $\kappa=\kappa_L+\kappa_R$ is the decay rate of the cavity, $\tilde{\Delta}\equiv\Delta+\sqrt{2}g_0Q_s$ is the effective detuning of the probe laser, $Q_s$ denotes the average mechanical displacement, and $g=g_0\bar{\alpha}$ is the cavity enhanced coupling rate. The optical noise operator injecting from the left (right) mirror is $\delta\hat{a}_{\text{in},L}(\delta\hat{a}_{\text{in},R})$. $\Gamma_m$ is the mechanical linewidth, and $\delta\hat{P}_{\rm in}$ is the mechanical momentum noise operator.

By introducing amplitude quadrature $\delta\hat{X}=\frac{\delta\hat{a}+\delta\hat{a}^\dagger}{\sqrt{2}}$ and phase quadrature $\delta\hat{Y}=\frac{\delta\hat{a}-\delta\hat{a}^\dagger}{\sqrt{2}i}$, Eq. (2) can be rewritten as

$$\begin{aligned}
\delta\dot{\hat{X}}&=-\frac{\kappa}{2}\delta\hat{X}-\tilde{\Delta}\delta\hat{Y}+\sqrt{\kappa_R}\delta\hat{X}_{\text{in},R}+\sqrt{\kappa_L}\delta\hat{X}_{\text{in},L},\\
\delta\dot{\hat{Y}}&=-\frac{\kappa}{2}\delta\hat{Y}+\tilde{\Delta}\delta\hat{X}+2g\delta\hat{Q}+\sqrt{\kappa_R}\delta\hat{Y}_{\text{in},R}+\sqrt{\kappa_L}\delta\hat{Y}_{\text{in},L},\\
\delta\dot{\hat{Q}}&=\Omega_m\delta\hat{P},\\
\delta\dot{\hat{P}}&=-\Omega_m\delta\hat{Q}-\Gamma_m\delta\hat{P}+\sqrt{2\Gamma_m}\delta\hat{P}_{\rm in}+2g\delta\hat{X},
\end{aligned} \tag{3}$$

where $\delta\hat{X}_{\text{in},j}=\frac{1}{\sqrt{2}}(\delta\hat{a}^\dagger_{\text{in},j}+\delta\hat{a}_{\text{in},j})$ and $\delta\hat{Y}_{\text{in},j}=\frac{i}{\sqrt{2}}(\delta\hat{a}^\dagger_{\text{in},j}-\delta\hat{a}_{\text{in},j})$, $j=\{L,R\}$, are the input amplitude and phase noise quadrature, respectively.

We assume $\tilde{\Delta}=0$, and the output probe field is measured by balanced homodyne detection (BHD). The measured

quadrature of the output probe field has the form

$$\hat{X}_{\text{out}} = \sqrt{\eta}(-\delta\hat{X}_{\text{in},L} + \sqrt{\kappa_L}\delta\hat{X}) + \sqrt{1-\eta}\delta\hat{X}_v,$$

$$\hat{Y}_{\text{out}} = \sqrt{\eta}(-\delta\hat{Y}_{\text{in},L} + \sqrt{\kappa}_L\delta\hat{Y}) + \sqrt{1-\eta}\delta\hat{Y}_v, \quad (4)$$

where $\eta$ denotes detection efficiency. Assuming that the quadrature with a phase angle of $\theta$ is measured in the frequency domain, we have

$$\hat{X}_\theta(\Omega) = \hat{X}_{\text{out}}(\Omega)\cos(\theta) + \hat{Y}_{\text{out}}(\Omega)\sin(\theta). \quad (5)$$

Here we assume that the squeezed light is generated from an optical parametrical amplifier (OPA), which can generate a high degree of quantum squeezing with current technology. By applying a phase shift operation of $\hat{U}(\phi) = e^{-i\phi\hat{n}}$ to the output of OPA, the squeezing angle $\phi$ can be manipulated, where $\hat{n} = \hat{a}^\dagger\hat{a}$ is an operator of the photon number. The effect of $\hat{U}(\phi)$ on the annihilation operator $\hat{a}$ is $\hat{U}^\dagger(\phi)\hat{a}\hat{U}(\phi) = \hat{a}e^{-i\phi}$. In this case, the input quadrature components of squeezed light to the optomechanical system are given by

$$\delta\hat{X}_{\text{in},L}(\Omega) = \cos(\phi)\hat{X}_o(\Omega) - \sin(\phi)\hat{Y}_o(\Omega),$$

$$\delta\hat{Y}_{\text{in},L}(\Omega) = \cos(\phi)\hat{Y}_o(\Omega) + \sin(\phi)\hat{X}_o(\Omega), \quad (6)$$

where $\hat{X}_o = \frac{1}{\sqrt{2}}(\hat{c}_o^\dagger + \hat{c}_o)$ and $\hat{Y}_o = \frac{i}{\sqrt{2}}(\hat{c}_o^\dagger - \hat{c}_o)$ are the amplitude and phase noise quadrature of the OPA output fields $\hat{c}_o$, respectively. The output field $\hat{c}_o$ satisfies the standard input–output relation

$$\hat{c}_o = \sqrt{\kappa_c}\hat{c} - \hat{c}_{\text{in}}, \quad (7)$$

where $\hat{c}$ denotes the OPA cavity mode, and the Langevin equation for the OPA has the form

$$\dot{\hat{c}} = -\frac{\kappa_o}{2}\hat{c} + \chi\hat{c}^\dagger + \sqrt{\kappa_c}\hat{c}_{\text{in}}, \quad (8)$$

where $\kappa_o$ is the decay rate of the OPA cavity, $\chi$ is the nonlinear interaction strength, $\kappa_c$ is the decay rate of the output OPA cavity mirror, and $\hat{c}_{\text{in}}$ denotes vacuum noise.

By using Eq. (7), Eq. (8), and the Wiener–Khinchin theorem $S_{\hat{R}\hat{R}} = \int_{-\infty}^{+\infty}\langle\hat{R}^\dagger(-\Omega)\hat{R}(\Omega')\rangle d\Omega'$, the output noise spectrum of the OPA can be obtained [35]:

$$S_{\hat{X}_o^\dagger\hat{X}_o}(\Omega) = \frac{1}{2} + \frac{\zeta\chi\kappa_o}{(\kappa_o-\chi)^2+\Omega^2},$$

$$S_{\hat{Y}_o^\dagger\hat{Y}_o}(\Omega) = \frac{1}{2} - \frac{\zeta\chi\kappa_o}{(\kappa_o+\chi)^2+\Omega^2},$$

$$S_{\hat{X}_o^\dagger\hat{Y}_o}(\Omega) = i/2,$$

$$S_{\hat{Y}_o^\dagger\hat{X}_o}(\Omega) = -i/2, \quad (9)$$

where $\Omega$ is analysis frequency, and $\zeta = \kappa_c/\kappa_o$ is the output coupling efficiency of the OPA. By introducing the normalized pumping parameter $\sigma = \sqrt{P_{\text{in}}/P_{\text{th}}}$ ($P_{\text{in}}$ is the pumping power of the pumping light, and $P_{\text{th}}$ is the threshold of the OPA) and normalized to the shot noise, anti-squeezing $V_a$ and squeezing $V_s$ can be written as

$$V_a = 1 + \frac{4\zeta\sigma}{(1-\sigma)^2 + \left(\frac{\Omega}{\kappa_c}\right)^2},$$

$$V_s = 1 - \frac{4\zeta\sigma}{(1+\sigma)^2 + \left(\frac{\Omega}{\kappa_c}\right)^2}. \quad (10)$$

Combining Eqs. (6) and (9), the noise spectrum of the input squeezing light to the optomechanical system is given by

$$S_{\hat{X}_{\text{in},L}^\dagger\hat{X}_{\text{in},L}}(\Omega) = \left(S_{\hat{X}_o^\dagger\hat{X}_o}\right)\cos^2(\phi) + \left(S_{\hat{Y}_o^\dagger\hat{Y}_o}\right)\sin^2(\phi),$$

$$S_{\hat{Y}_{\text{in},L}^\dagger\hat{Y}_{\text{in},L}}(\Omega) = \left(S_{\hat{X}_o^\dagger\hat{X}_o}\right)\sin^2(\phi) + \left(S_{\hat{Y}_o^\dagger\hat{Y}_o}\right)\cos^2(\phi),$$

$$S_{\hat{X}_{\text{in},L}^\dagger\hat{Y}_{\text{in},L}}(\Omega) = i/2 + \sin(\phi)\cos(\phi)\left(S_{\hat{X}_o^\dagger\hat{X}_o} - S_{\hat{Y}_o^\dagger\hat{Y}_o}\right),$$

$$S_{\hat{Y}_{\text{in},L}^\dagger\hat{X}_{\text{in},L}}(\Omega) = -i/2 + \sin(\phi)\cos(\phi)\left(S_{\hat{X}_o^\dagger\hat{X}_o} - S_{\hat{Y}_o^\dagger\hat{Y}_o}\right). \quad (11)$$

The symmetrized power spectral density (PSD) of an operator $\hat{R}$ is defined as

$$\bar{S}_{\hat{R}\hat{R}}(\Omega) = \frac{S_{\hat{R}\hat{R}}(\Omega) + S_{\hat{R}\hat{R}}(-\Omega)}{2}. \quad (12)$$

Supposing our system is in steady state, $\bar{S}_{X_\theta X_\theta}$ can be calculated by using the Wiener–Khinchin theorem, and $\bar{S}_{X_\theta X_\theta}$ can be derived:

$$\begin{aligned}\bar{S}_{X_\theta X_\theta}(\Omega) &= \bar{S}_{Q_{\text{det}}Q_{\text{det}}}(\Omega)\, f_{\text{imp}}(\Omega) \\ &= [\bar{S}_{\text{imp}}(\Omega) + \bar{S}_{QQ}(\Omega) + \bar{S}_{\text{cor}}(\Omega)]\, f_{\text{imp}}(\Omega), \quad (13)\end{aligned}$$

where $f_{\text{imp}}(\Omega) = 2\eta\eta_c\Gamma_m|C_{\text{eff}}(\Omega)|[1-\cos(2\theta)]$ is the transfer function between the displacement spectrum $\bar{S}_{Q_{\text{det}}Q_{\text{det}}}$ and optical quadrature spectrum $\bar{S}_{X_\theta X_\theta}$ with the effective optomechanical cooperativity $|C_{\text{eff}}| \equiv 4g^2/[\kappa\Gamma_m|1-2i\Omega/\kappa|^2)]$, and $\eta_c = \kappa_L/\kappa$. The first item of the right side of Eq. (13) serves as imprecision noise in the PSD. The second term represents the mechanical oscillator's displacement spectrum $\bar{S}_{QQ}$, which is given by

$$\bar{S}_{QQ} = |\chi_m|^2(\bar{S}_{qba} + \bar{S}_{\text{th}}), \quad (14)$$

where $\chi_m(\Omega) = \Omega_m/[(\Omega_m^2 - \Omega^2) - i\Gamma_m\Omega]$ is the dimensionless mechanical susceptibility. $\bar{S}_{qba}$ is quantum backaction noise, which arises from the effect of random arrival of probe photons on the mirror. $\bar{S}_{\text{th}}$ is thermal noise caused by the exchange between the resonator and thermal environment. The third term $S_{\text{cor}}$ represents quantum correlations between imprecision and backaction.

Using the results of Eq. (11) and the quantum fluctuation–dissipation theorem, we can write Eq. (15), which is the explicit expressions of each term in Eq. (13):

$$\bar{S}_{\mathrm{imp}}(\Omega)=\frac{1}{2f_{\mathrm{imp}}}+\frac{\kappa(\eta_c-1)F_1}{2g^2[1-\cos(2\theta)]}+\frac{\eta F_1}{f_{\mathrm{imp}}},$$

$$\bar{S}_{QQ}(\Omega)=|\chi_m|^2\left[2\Gamma_m|C_{\mathrm{eff}}|+4\Gamma_m|C_{\mathrm{eff}}|\eta_c F_2+2\Gamma_m\left(n_{\mathrm{th}}+\frac{1}{2}\right)\right],$$

$$\bar{S}_{\mathrm{cor}}(\Omega)=\frac{R_e[\chi_m]}{\tan(\theta)}+\frac{8g^2\eta\kappa_L F_3 R_e[F_4]\sin(\theta)}{f_{\mathrm{imp}}},$$

$$F_1=S_{\hat{X}_o^\dagger\hat{X}_o}\cos^2(\theta-\phi)+S_{\hat{Y}_o^\dagger\hat{Y}_o}\sin^2(\theta-\phi)-\frac{1}{2},$$

$$F_2=S_{\hat{X}_o^\dagger\hat{X}_o}\cos^2(\phi)+S_{\hat{Y}_o^\dagger\hat{Y}_o}\sin^2(\phi)-\frac{1}{2},$$

$$F_3=\cos(\phi)\cos(\theta-\phi)\left(S_{\hat{X}_o^\dagger\hat{X}_o}-\frac{1}{2}\right)-\sin(\phi)\sin(\theta-\phi)\left(S_{\hat{Y}_o^\dagger\hat{Y}_o}-\frac{1}{2}\right),$$

$$F_4=\frac{\chi_m}{\frac{\kappa}{2}-i\omega}\left(\frac{\kappa_L}{\left(\frac{\kappa}{2}\right)^2+\omega^2}-\frac{1}{\frac{\kappa}{2}-i\omega}\right). \tag{15}$$

By inserting $S_{\hat{X}_o^\dagger\hat{X}_o}(\Omega)=S_{\hat{Y}_o^\dagger\hat{Y}_o}(\Omega)=\frac{1}{2}$ into Eq. (13), we can recover the results of coherent light driving. Notice that the optomechanical SQL results from a balance between the optical shot noise and radiation pressure noise; the added detection noise reaches the SQL $\bar{S}_{\mathrm{SQL}}=|\chi_m|$ under the condition of effective cooperativity $|C_{\mathrm{eff}}^{\mathrm{opt}}|=1/(4\Gamma_m|\chi_m(\Omega)|)$.

In the following, we will use Eqs. (13) and (15) to analyze the mechanical displacement spectrum with variational readout and squeezed light injection.

## 3. EFFECT OF SYSTEM PARAMETERS ON DISPLACEMENT MEASUREMENT BEYOND THE SQL

It can be seen from Eqs. (13) and (15) that the displacement spectrum depends on the optomechanical coupling strength $g$, squeezing level $V_s$, squeezing angle $\phi$, and measurement angle $\theta$. Optomechanical coupling strength $g$ can be tuned by adjusting the input power of the probe light $P_{\mathrm{det}}$. To ensure that the system stably works in the linear region of the F-P cavity, the probe optical power is confined to a certain range [36]. To maximize displacement measurement sensitivity at the far detuning frequency, the squeezing level $V_s$, probe power $P_{\mathrm{det}}$, squeezing angle $\phi$, and measurement angle $\theta$ should be optimized, as shown in Fig. 2.

Figure 2 shows the off-resonant displacement sensitivity under different measurement conditions. When a coherent probe is used, displacement sensitivity reaches 2.6 dB (black circles) below the SQL at a sideband frequency of $\Omega=\Omega_m+4000\,\Gamma_m$. When a probe light with a fixed squeezing angle combines with optimal measurement angle, phase quadrature squeezed light (green line) is superior to amplitude quadrature squeezed light (magenta line) at the far-detuned detection frequency. If a squeezed probe with optimal squeezing angle combines with a fixed measurement angle, displacement sensitivity can improve

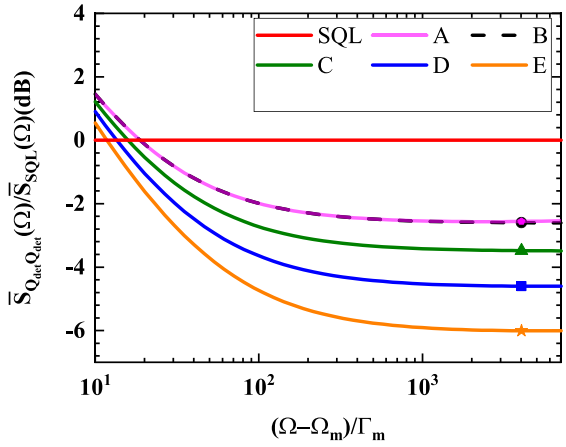


**Fig. 2.** Displacement spectra under different measurement conditions with LOC and squeezed light injection; $P_{\mathrm{opt}}$, $V_{\mathrm{sopt}}$, $\theta_{\mathrm{opt}}$, and $\phi_{\mathrm{opt}}$ represent the optimal probe power, squeezing level, measurement angle, and squeezing angle, respectively. The symbols on the curves denote the frequency of $(\Omega-\Omega_m)/\Gamma_m=4037$. Curve A denotes squeezed light with $P_{\mathrm{det}}=P_{\mathrm{opt}}$, $V_s=V_{\mathrm{sopt}}$, $\theta=\theta_{\mathrm{opt}}$, and $\phi=\pi/2$; curve B denotes coherent light with $P_{\mathrm{det}}=P_{\mathrm{opt}}$ and $\theta=\theta_{\mathrm{opt}}$; curve C denotes squeezed light with $P_{\mathrm{det}}=P_{\mathrm{opt}}$, $V_s=V_{\mathrm{sopt}}$, $\theta=\theta_{\mathrm{opt}}$, and $\phi=0$; curve D denotes squeezed light with $P_{\mathrm{det}}=P_{\mathrm{opt}}$, $V_s=V_{\mathrm{sopt}}$, $\theta=\pi/2$, and $\phi=\phi_{\mathrm{opt}}$; curve E denotes squeezed light with $P_{\mathrm{det}}=P_{\mathrm{opt}}$, $V_s=V_{\mathrm{sopt}}$, $\theta=\theta_{\mathrm{opt}}$, and $\phi=\phi_{\mathrm{opt}}$. Other simulation parameters are $\eta=0.81$, $\eta_c=0.95$, $\zeta=0.85$, $\kappa_o=2\pi\times10$ MHz, $\Omega_m=2\pi\times1.135$ MHz, $\kappa=2\pi\times16.2$ MHz, $\Gamma_m=2\pi\times32$, $g_0=2\pi\times120.7$, $\lambda=1064$ nm, and $n_{\mathrm{th}}=8$ [17].

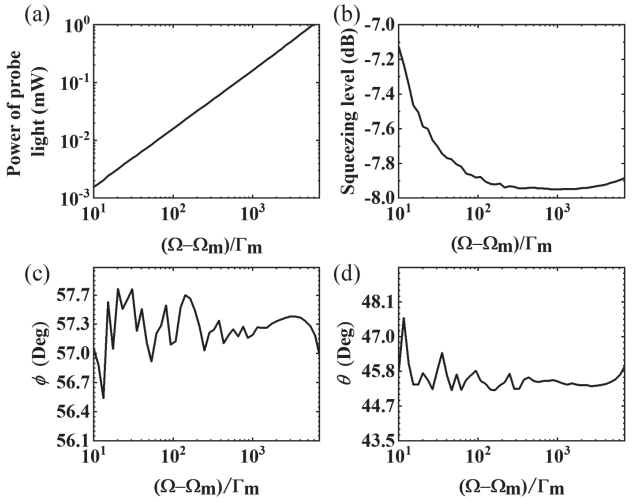


**Fig. 3.** Optimal system parameters versus the normalized analysis frequency with squeezed light injection and variational readout under the condition of global optimization.

to 4.6 dB below the SQL (blue square). In contrast, sensitivity can reach 6 dB (orange star) below the SQL when all parameters $(P_{\mathrm{det}}, V_s, \phi, \theta)$ are globally optimized.

Figure 3 shows the optimal choices of the power of the probe light, squeezing level, squeezing angles, and measurement angles of homodyne detection, under the condition of global optimization. Because the mechanical response $\chi_m$ shows a Lorentz distribution, the backaction noise decreases with the detuning of the analysis frequency, so that the optimal power of the probe

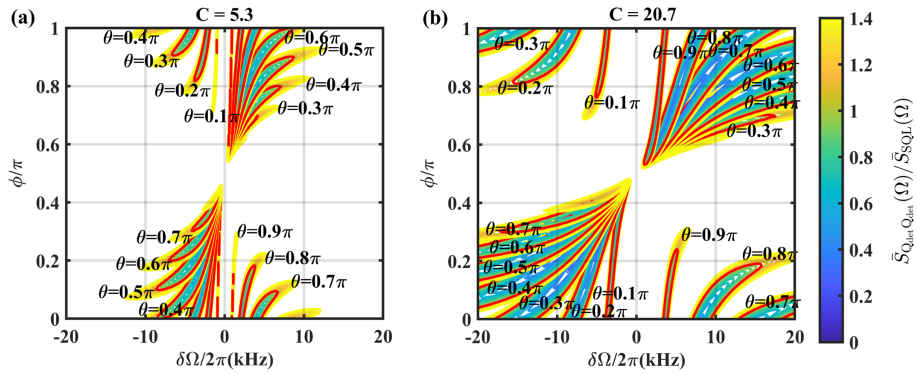


**Fig. 4.** Sub-SQL sensitivity versus squeezing angle and measurement frequency (other parameters are fixed). Red contour lines correspond to $\bar{S}_{\mathrm{SQL}}$ and $\delta\Omega = \Omega - \Omega_m$. Pumping parameter $\sigma = 0.77$. Other simulation parameters are the same as those in Fig. 2.

light increases with the detuning of measurement frequency [Fig. 3(a)]. Figure 3(b) indicates that the optimal squeezing level increases with the analysis frequency and then tends to flatten out. The optimal squeezing angle and measurement angle fluctuate within 2 deg. This implies that once the experimental system is given, only the squeezing level and the optical power of the probe light need to be adjusted along with the analysis frequency in the frequency range from $(\Omega - \Omega_m)/\Gamma_m = 10$ to 8000.

In Fig. 2, we analyze the sub-SQL performance of displacement measurement when four relevant parameters are globally optimized. When the measurement strength $C = 4g^2/\kappa\Gamma_m$ and squeezing level are fixed, the influence of the other parameters (squeezing angle and measurement angle) on sensitivity is shown in Fig. 4. It is clear that the best squeezing angle changes from the amplitude quadrature to phase quadrature as the measurement frequency varies from the low-frequency to high-frequency region. Comparing Figs. 4(a) and 4(b), where different measurement strengths with $C = 5.3$, 20.7 are assumed, we find that the bandwidth of the sub-SQL performance is improved for larger $C$. Therefore, one can achieve ultrasensitive measurement at a wider range of frequencies by increasing the measurement strength $C$, which can be adjusted by the probe power.

Figure 5 shows the normalized displacement PSD as a function of the squeezing angle and measurement angle at a non-perfect measurement efficiency of $\eta = 0.81$. We see that the squeezing angle has a nonlinear dependence on the measurement angle for the region where the SQL is surpassed at the fixed probe power, squeezing level $V_s$, and analysis frequency. When the measurement intensity $C$ is enhanced, the nonlinear dependence between the squeezing angle and measurement angle is increased.

Next, we analyze the effects of various system losses on measurement sensitivity. For a coherent state probe field, high-input coupling efficiency $\eta_c$ and detection efficiency $\eta$ are always beneficial to the displacement measurement. However, when squeezing light is used, there exists an optimal detection efficiency in general when the other system parameters are fixed and the pump parameter $\sigma$ is large, as shown in Fig. 6. This is because the large pump parameter $\sigma$ results in large anti-squeezed noise, which significantly increases the backaction

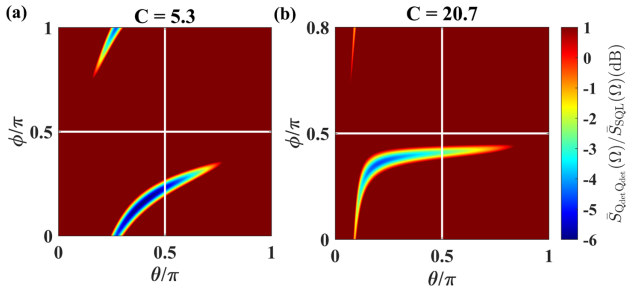


**Fig. 5.** Displacement power spectral density as a function of squeezing angle $\phi$ and measurement angle $\theta$ at sideband frequency of $\Omega - \Omega_m = 100\ \Gamma_m$. SQL can be surpassed by (a) 3.2 dB and (b) 4.6 dB, respectively. Pumping parameter $\sigma = 0.77$. Other simulation parameters are the same as those in Fig. 2.

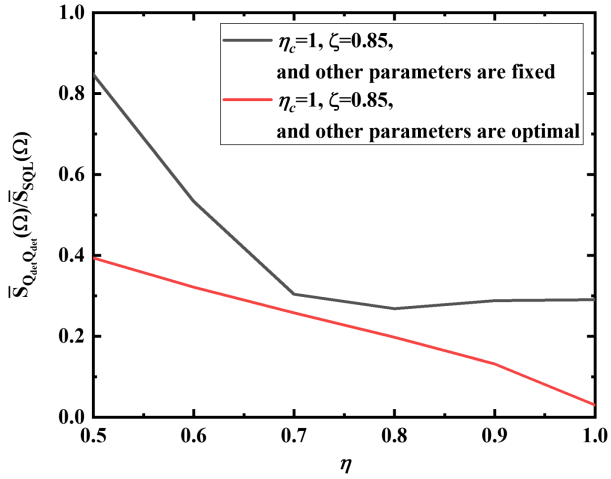


**Fig. 6.** Displacement sensitivity versus measurement efficiency $\eta$ at $\Omega - \Omega_m = 8 \times 10^3\ \Gamma_m$. Parameters for the black line are $\sigma = 0.85$, $P_{\mathrm{det}} = 1.4$ mW, $\theta = 0.26\pi$, and $\phi = 0.31\pi$. Other simulation parameters are the same as those in Fig. 2.

noise. In this case, the small reduction in detection efficiency can effectively suppress the backaction noise despite that it increases the impression noise a little. In contrast, when the other parameters are optimized, the perfect detection efficiency $\eta$ is always best for the displacement measurement.

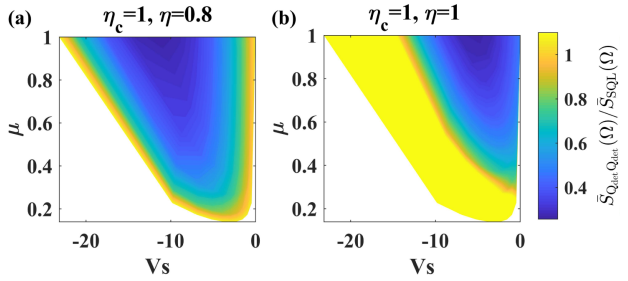


**Fig. 7.** Displacement sensitivity versus purity and squeezing level $V_s$ of the probe light at $\Omega - \Omega_m = 8 \times 10^3\,\Gamma_m$. The white area depicts the parameter space that cannot be reached by arranging the pump parameter $\sigma$ and escape efficiency $\zeta$. $P_{\rm det} = 1.4$ mW, $\theta = 0.26\pi$, $\phi = 0.31\pi$, and other simulation parameters are the same as those in Fig. 2.

The squeezing level and purity of squeezed light also affect the performance of displacement measurement sensitivity. The purity of a single mode squeezed state is directly related to its squeezing and anti-squeezing, given by [37]

$$\mu = T_r[\rho^2] = 2\pi \iint W(\hat{x}, \hat{p})\mathrm{d}x\mathrm{d}p = \frac{1}{\sqrt{V_a V_s}}. \tag{16}$$

By varying the pump parameter $\sigma \in [0, 1]$ and escape efficiency $\zeta \in [0, 1]$ of the OPA and using Eq. (16), we can obtain a series of squeezing levels and purity pairs $[\sigma, \zeta]$. Given $\eta_c$ and $\eta$, the displacement measurement versus squeezing level and purity of squeezed light is depicted in Fig. 7 (for each point, the probe power is fixed). We see that high purity is always helpful for sensitivity, and there is an optimal squeezing for a given purity. For higher $\eta_c$ and $\eta$, the optimal squeezing level is lower, and only moderate squeezing of 5 dB is required when $\eta_c = \eta = 1$ as shown in Fig. 7(b).

## 4. DISPLACEMENT MEASUREMENT WITH NONLINEAR OPTOMECHANICAL COUPLING AND SQUEEZED LIGHT INJECTION

In previous sections, we have studied the displacement measurement beyond SQL with LOC and variational readout with squeezed light. In this section, we go beyond the LOC interaction by introducing the QOC into the optomechanical system, and derive the displacement measurement spectrum with nonlinear optomechanical coupling and variational readout with squeezed light. In this case, the Hamiltonian of the system is given by

$$\hat{H}_q = \frac{\hbar\Omega_m}{2}(\hat{Q}^2 + \hat{P}^2) - \hbar\Delta\hat{a}^\dagger\hat{a} - \sqrt{2}\hbar\hat{a}^\dagger\hat{a}\,\hat{Q}(g_0 + \sqrt{2}g_q\,\hat{Q}) + i\hbar\sqrt{\kappa_L}(\alpha_{\rm in}\hat{a}^\dagger + \mathrm{c.c}), \tag{17}$$

where $g_q$ describes the vacuum QOC rate. We simulate the dynamics of the system by expanding the field operators as the steady-state values and fluctuation terms as mentioned above. Then we get the steady state solutions of the fields: $\bar{\alpha} = \sqrt{\eta_c\kappa}\bar{\alpha}_{{\rm in},L}/[\kappa/2 - i(\tilde{\Delta} + 2g_q Q_s^2)]$ and $Q_s = (-g_l|\bar{\alpha}|^2)/(\Omega_m + 2g_q|\bar{\alpha}|^2)$. By neglecting the small quantities, the Langevin equations of the fluctuations are given by

$$\begin{aligned}
\delta\dot{\hat{X}} &= -\frac{\kappa}{2}\delta\hat{X} - B\delta\hat{Y} - \tilde{G}Y_s\delta\hat{Q} + \sqrt{\kappa_R}\delta\hat{X}_{{\rm in},R} + \sqrt{\kappa_L}\delta\hat{X}_{{\rm in},L},\\
\delta\dot{\hat{Y}} &= -\frac{\kappa}{2}\delta\hat{Y} + B\delta\hat{X} + \tilde{G}X_s\delta\hat{Q} + \sqrt{\kappa_R}\delta\hat{Y}_{{\rm in},R} + \sqrt{\kappa_L}\delta\hat{Y}_{{\rm in},L},\\
\delta\dot{\hat{Q}} &= \Omega_m\delta\hat{P},\\
\delta\dot{\hat{P}} &= -\tilde{\Omega}_m\delta\hat{Q} - \Gamma_m\delta\hat{P} + \tilde{G}X_s\delta\hat{X} + \tilde{G}Y_s\delta\hat{Y} + \sqrt{2\Gamma_m}\delta\hat{P}_{\rm in},
\end{aligned} \tag{18}$$

where

$$\begin{aligned}
B &\equiv \tilde{\Delta} + 2g_q Q_s^2,\\
\tilde{\Omega}_m &\equiv \Omega_m - 4g_q|\bar{\alpha}|^2,\\
\tilde{G} &\equiv \sqrt{2}g_0 + 4g_q Q_s,\\
X_s &= \frac{\bar{\alpha} + \bar{\alpha}^*}{\sqrt{2}},\ Y_s = \frac{\bar{\alpha} - \bar{\alpha}^*}{\sqrt{2}i}.
\end{aligned} \tag{19}$$

We assume that $B = 0$, which means $Y_s = 0$. We choose negative QOC to achieve higher measurement sensitivity because the system must be physical ($\frac{\tilde{\Omega}_m}{\Omega_m} = 1 - \frac{2g_q|\bar{\alpha}|^2}{\Omega_m} > 0$).

Starting from Eqs. (20) and (11), we can get the mechanical displacement spectrum under the condition of combined LOC and QOC with variational readout and squeezed light injection:

$$\begin{aligned}
\bar{S}'_{X_\theta X_\theta}(\Omega) &= \bar{S}'_{Q_{\rm det}Q_{\rm det}}(\Omega)\,f'_{\rm imp}(\Omega)\\
&= [\bar{S}'_{\rm imp}(\Omega) + \bar{S}'_{QQ}(\Omega) + \bar{S}'_{\rm cor}(\Omega)]\,f'_{\rm imp}(\Omega),
\end{aligned} \tag{20}$$

where $f'_{\rm imp}(\Omega) = 2\eta\eta_c\Gamma_m|C_{\rm eff2}(\Omega)|[1 - \cos(2\theta)]$ is the transfer function between the displacement spectrum $\bar{S}'_{Q_{\rm det}Q_{\rm det}}$ and optical quadrature spectrum $\bar{S}'_{X_\theta X_\theta}$ with the effective optomechanical cooperativity of $|C_{\rm eff2}| \equiv \tilde{G}^2X_s^2/[\kappa\Gamma_m|1 - 2i\Omega/\kappa|^2)]$:

$$\begin{aligned}
\bar{S}'_{\rm imp}(\Omega) &= \frac{1}{2f'_{\rm imp}} + \frac{2\kappa(\eta_c - 1)F_1}{X_s^2\tilde{G}^2[1 - \cos(2\theta)]} + \frac{\eta F_1}{f'_{\rm imp}},\\
\bar{S}'_{QQ}(\Omega) &= |\chi_{\rm eff}|^2\Big[2\Gamma_m|C_{\rm eff2}| + 4\Gamma_m|C_{\rm eff2}|\eta_c F_2\\
&\quad + 2\Gamma_m\left(n_{\rm th} + \frac{1}{2}\right)\Big],\\
\bar{S}'_{\rm cor}(\Omega) &= \frac{R_e[\chi_{\rm eff}]}{\tan(\theta)} + \frac{\kappa\tilde{G}^2X_s^2F_3R_e[F_4]}{2\Gamma_m|C_{\rm eff2}|\sin(\theta)}.
\end{aligned} \tag{21}$$

Comparing Eq. (21) with Eq. (15), we find that $\tilde{G}^2X_s^2$ take the place of $4g^2$. When $g_q = 0$, the optomechanical system returns to LOC interaction. $\chi_{\rm eff}(\Omega) = \Omega_m/[(\Omega_m\tilde{\Omega}_m - \Omega^2) - i\Gamma_m\Omega]$ is the effective dimensionless mechanical susceptibility. The presence of negative QOC affects both the resonance frequency of the resonator $\Omega_{\rm eff} = \sqrt{\Omega_m\tilde{\Omega}_m}$ and the mechanical spring constant $K_{\rm eff} = m\Omega_m\tilde{\Omega}_m$. Because of $\tilde{\Omega}_m > \Omega_m$, we have

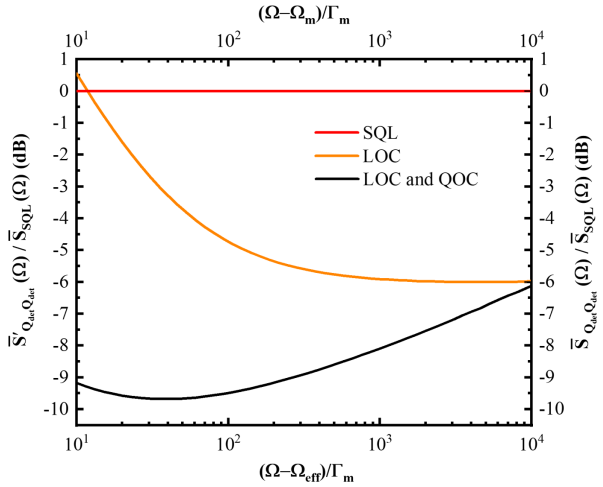


**Fig. 8.** Displacement spectrum under the condition of nonlinear optomechanical coupling (combined LOC and QOC) and squeezed light injection.

$\Omega_{\mathrm{eff}} > \Omega_m$ and $K_{\mathrm{eff}} > K = \tilde{\Omega}_m \Omega_m$, which means a stiffer mode is generated [32].

Figure 8 illustrates the displacement spectrum under the condition of nonlinear optomechanical coupling (combined LOC and QOC) and squeezed light injection. The relevant parameters including the power of the probe light, squeezing level, squeezing angles, QOC rate, and readout quadrature are globally optimized. It is clear that the introduction of QOC interaction significantly improve displacement sensitivity, which can reach 9.6 dB below the SQL at an analysis frequency of $(\Omega - \Omega_{\mathrm{eff}})/\Gamma_m = 30$, and the required QOC rate is $g_q/g_l = -1.8 \times 10^{-4}$. In combining LOC and QOC optomechanical systems, the smaller effective coupling rate $\tilde{G}$ together with the larger spring constant $K_{\mathrm{eff}}$ diminishes the backaction noise level at the price of higher probe power. The optimal balance of backaction noise, thermal noise, imprecision noise, and quantum correlation between backaction noise and imprecision noise eventually leads to lower total displacement noise.

## 5. CONCLUSION

We established an ultrasensitive displacement measurement model to overcome the SQL in the unresolved sideband cavity optomechanical system with nonlinear optomechanical coupling and squeezed light injection. Key parameters including the squeezing angle, squeezing level, probe optical power, readout quadrature, and various losses of the system on displacement measurement sensitivity and their interplay were analyzed in depth. The appropriate matching between the squeezed angle and readout quadrature is critical to effectively suppress impresicion noise and backaction noise. In contrast to the coherent state probe where perfect detection is desired to improve sensitivity, we find that the higher detection efficiency does not necessarily result in better measurement sensitivity due to the antisqueezing noise of the squeezing light, and an optimal detection efficiency exists in general when the other conditions are fixed. High purity of the squeezed probe is always beneficial to sensitivity, and there is an optimal squeezing level for a given purity. For higher detection efficiency and input coupling efficiency of the optomechanical system, the optimal squeezing level is lower. Furthermore, the combined LOC and QOC can significantly improve displacement sensitivity since a stiffer mode is induced.

Our results are useful for the design and parameter optimization of the displacement measurement in the unresolved sideband cavity optomechanical system. The proposed approach may find applications in gravitational detectors to enhance sensitivity [38] and increase detection sensitivity in feedback cooling and thus decrease the final phonon occupancy [39–41]. The variational readout is compatible with the state-of-the-art force-sensing application [42], and our method is also helpful to improve force-sensing sensitivity.

**Funding.** National Natural Science Foundation of China (11774209, 11804208, 12174232, 62175138); Shanxi 1331 KSC.

**Disclosures.** The authors declare no conflicts of interest.

**Data availability.** Data underlying the results presented in this paper are not publicly available at this time but may be obtained from the authors upon reasonable request.

## REFERENCES

1. W. P. Bowen and G. J. Milburn, "Linear quantum measurement of mechanical motion," in *Quantum Optomechanics* (CRC Press/Taylor and Francis Group, 2016), p. 77.
2. A. B. Matsko and S. P. Vyatchanin, "Standard quantum limit of sensitivity of an optical gyroscope," Phys. Rev. A **98**, 063821 (2018).
3. M. R. Mason, J. Chen, Y. Tsaturyan, and A. Schliesser, "Measurement-based quantum control of mechanical motion," Nature **563**, 53–58 (2018).
4. B. J. Lawrie, P. D. Lett, A. M. Marino, and R. C. Pooser, "Quantum sensing with squeezed light," ACS Photon. **6**, 1307–1318 (2019).
5. J. B. Clark, F. Lecocq, R. W. Simmonds, J. Aumentado, and J. D. Teufel, "Observation of strong radiation pressure forces from squeezed light on a mechanical oscillator," Nat. Phys. **12**, 683–687 (2016).
6. S. Schreppler, N. Spethmann, N. Brahms, T. Botter, M. Barrios, and D. M. Stamper-Kurn, "Optically measuring force near the standard quantum limit," Science **344**, 1486–1489 (2014).
7. The LIGO Scientific Collaboration, "Enhanced sensitivity of the LIGO gravitational wave detector by using squeezed states of light," Nat. Photonics **7**, 613–619 (2013).
8. E. Zeuthen, E. S. Polzik, and F. Y. Khalili, "Gravitational wave detection beyond the standard quantum limit using a negative-mass spin system and virtual rigidity," Phys. Rev. D **100**, 062004 (2019).
9. The LIGO Scientific Collaboration, "A gravitational wave observatory operating beyond the quantum shot-noise limit," Nat. Phys. **7**, 962–965 (2011).
10. M. A. Page, M. Goryachev, H. Miao, Y. Chen, Y. Ma, D. Mason, M. Rossi, C. D. Blair, L. Ju, D. G. Blair, A. Schliesser, M. E. Tobar, and C. Zhao, "Gravitational wave detectors with broadband high frequency sensitivity," Commun. Phys. **4**, 27 (2021).
11. H. Yu, L. McCuller, M. Tse, N. Kijbunchoo, L. Barsotti, N. Mavalvala, and L. S. Collaboration, "Quantum correlations between light and the kilogram-mass mirrors of LIGO," Nature **583**, 43–47 (2020).
12. M. Tse, H. Yu, and N. Kijbunchoo, "Quantum-enhanced advanced ligo detectors in the era of gravitational-wave astronomy," Phys. Rev. Lett. **123**, 231107 (2019).
13. D. Carney, G. Krnjaic, D. C. Moore, *et al.*, "Mechanical quantum sensing in the search for dark matter," Quantum Sci. Technol. **6**, 024002 (2021).
14. V. B. Braginsky, Y. Vorontsov, and K. S. Thorne, "Quantum nondemolition measurements," Science **209**, 547–557 (1980).
15. C. B. Møller, R. A. Thomas, G. Vasilakis, E. Zeuthen, Y. Tsaturyan, M. Balabas, K. Jensen, A. Schliesser, K. Hammerer, and E. S. Polzik, "Quantum back-action-evading measurement of motion in a negative mass reference frame," Nature **547**, 191–195 (2017).

16. N. S. Kampel, R. W. Peterson, R. Fischer, P.-L. Yu, K. Cicak, R. W. Simmonds, K. W. Lehnert, and C. A. Regal, "Improving broadband displacement detection with quantum correlations," Phys. Rev. X **7**, 021008 (2017).
17. D. Mason, J. Chen, M. Rossi, Y. Tsaturyan, and A. Schliesser, "Continuous force and displacement measurement below the standard quantum limit," Nat. Phys. **15**, 745–749 (2019).
18. C. Laflamme and A. A. Clerk, "Quantum-limited amplification with a nonlinear cavity detector," Phys. Rev. A **83**, 033803 (2011).
19. M. J. Yap, J. Cripe, G. L. Mansell, T. G. McRae, R. L. Ward, B. J. J. Slagmolen, P. Heu, D. Follman, G. D. Cole, T. Corbitt, and D. E. McClelland, "Broadband reduction of quantum radiation pressure noise via squeezed light injection," Nat. Photonics **14**, 19–23 (2020).
20. S. S. Y. Chua, B. J. J. Slagmolen, D. A. Shaddock, and D. E. McClelland, "Quantum squeezed light in gravitational-wave detectors," Class. Quantum Gravity **31**, 183001 (2014).
21. C.-W. Lee, J. H. Lee, and H. Seok, "Squeezed-light-driven force detection with an optomechanical cavity in a Mach-Zehnder interferometer," Sci. Rep. **10**, 17496 (2020).
22. W. Li, Y. Jin, X. Yu, and J. Zhang, "Enhanced detection of a low-frequency signal by using broad squeezed light and a bichromatic local oscillator," Phys. Rev. A **96**, 023808 (2017).
23. M. Asjad, S. Zippilli, and D. Vitali, "Suppression of stokes scattering and improved optomechanical cooling with squeezed light," Phys. Rev. A **94**, 051801 (2016).
24. Y. Zhao, N. Aritomi, E. Capocasa, *et al.*, "Frequency-dependent squeezed vacuum source for broadband quantum noise reduction in advanced gravitational-wave detectors," Phys. Rev. Lett. **124**, 171101 (2020).
25. S. Vyatchanin and E. Zubova, "Quantum variation measurement of a force," Phys. Lett. A **201**, 269–274 (1995).
26. H. J. Kimble, Y. Levin, A. B. Matsko, K. S. Thorne, and S. P. Vyatchanin, "Conversion of conventional gravitational-wave interferometers into quantum nondemolition interferometers by modifying their input and/or output optics," Phys. Rev. D **65**, 022002 (2001).
27. H. Kerdoncuff, U. B. Hoff, G. I. Harris, W. P. Bowen, and U. L. Andersen, "Squeezing-enhanced measurement sensitivity in a cavity optomechanical system," Ann. Phys. **527**, 107–114 (2015).
28. W. J. Gu, Y. Y. Wang, Z. Yi, W.-X. Yang, and L. H. Sun, "Force measurement in squeezed dissipative optomechanics in the presence of laser phase noise," Opt. Express **28**, 12460–12474 (2020).
29. T. Zhang, J. Bentley, and H. Miao, "A broadband signal recycling scheme for approaching the quantum limit from optical losses," Galaxies **9**, 3 (2021).
30. J. D. Thompson, B. M. Zwickl, A. M. Jayich, F. Marquardt, S. M. Girvin, and J. G. E. Harris, "Strong dispersive coupling of a high-finesse cavity to a micromechanical membrane," Nature **452**, 72–75 (2008).
31. U. S. Sainadh and M. A. Kumar, "Force sensing beyond standard quantum limit with optomechanical "soft" mode induced by nonlinear interaction," Opt. Lett. **45**, 619–622 (2020).
32. U. S. Sainadh and M. A. Kumar, "Displacement sensing beyond the standard quantum limit with intensity-dependent optomechanical coupling," Phys. Rev. A **102**, 063523 (2020).
33. S. Fedorov, V. Sudhir, R. Schilling, H. Schütz, D. Wilson, and T. Kippenberg, "Evidence for structural damping in a high-stress silicon nitride nanobeam and its implications for quantum optomechanics," Phys. Lett. A **382**, 2251–2255 (2018).
34. A. Barg, Y. Tsaturyan, E. Belhage, W. H. P. Nielsen, C. B. Møller, and A. Schliesser, "Measuring and imaging nanomechanical motion with laser light," Appl. Phys. B **123**, 8 (2017).
35. P. K. Lam, T. C. Ralph, B. C. Buchler, D. McClelland, H.-A. Bachor, and J. Gao, "Optimization and transfer of vacuum squeezing from an optical parametric oscillator," J. Opt. **B1**, 469 (1999).
36. P. Meystre, E. M. Wright, J. D. McCullen, and E. Vignes, "Theory of radiation-pressure-driven interferometers," J. Opt. Soc. Am. B **2**, 1830–1840 (1985).
37. G. Breitenbach, S. Schiller, and J. Mlynek, "Measurement of the quantum states of squeezed light," Nature **387**, 471–475 (1997).
38. S. Vyatchanin and A. Matsko, "On sensitivity limitations of a dichromatic optical detection of a classical mechanical force," J. Opt. Soc. Am. B **35**, 1970–1978 (2017).
39. H. Habibi, E. Zeuthen, M. Ghanaatshoar, and K. Hammerer, "Quantum feedback cooling of a mechanical oscillator using variational measurements: tweaking Heisenberg's microscope," J. Opt. **18**, 084004 (2016).
40. The LIGO Scientific Collaboration, "Approaching the motional ground state of a 10-kg object," Science **372**, 1333–1336 (2021).
41. C. Schäfermeier, H. Kerdoncuff, U. B. Hoff, H. Fu, A. Huck, J. Bilek, G. I. Harris, W. P. Bowen, T. Gehring, and U. L. Andersen, "Quantum enhanced feedback cooling of a mechanical oscillator using nonclassical light," Nat. Commun. **7**, 13628 (2016).
42. M. Poggio and C. Degen, "Force-detected nuclear magnetic resonance: recent advances and future challenges," Nanotechnology **21**, 342001 (2010).